

### CHAPTER 3

## DIPOLAR-COUPPLING-MEDIATED COHERENCE TRANSFER IN A HOMONUCLEAR TWO SPIN $\frac{1}{2}$ SOLID STATE SYSTEM

### Abstract

Homonuclear dipolar-mediated coherence transfer (DCT), a through-space transfer of magnetization between like spins, can yield otherwise difficult-to-obtain structural information for macromolecules by measuring the internuclear distances between two sites of interest. The behavior of a spin- $\frac{1}{2}$  system under DCT is analyzed in detail by computing the time development of the density matrix using the product operator formalism. The effect of coherence transfer (CT) via the homonuclear isotropic scalar coupling on DCT is examined. Analytical and computational results that yield useful information on the frequencies, first-maxima, and first-zero of CT for a uniaxially oriented or a single-crystal solid-state system are presented. The results predict that the evolution of the spin angular momentum operators under the homonuclear dipolar coupling Hamiltonian leads to “cylindrical mixing” unlike “isotropic mixing” due to the strong scalar coupling Hamiltonian. These results will find relevance in both the design of RF pulse sequences for the structural studies of uniaxially oriented biological solids and the interpretation of solution NMR results from proteins embedded in partially oriented bicelles.

## Introduction

The phenomenon of exchange of nuclear spin magnetization through direct and indirect spin-spin interaction is known as polarization transfer or magnetization transfer or Hartmann-Hahn cross-polarization in NMR spectroscopy [41]. In this paper, we prefer to use the term “coherence transfer” (CT) to represent this phenomenon as it is a general term which defines the transfer of single-quantum coherence (or magnetization or polarization) and multiple-quantum coherences. CT via the scalar coupling (also known as indirect coupling or through-bond coupling or J coupling) is the basic concept behind many successful solution NMR experiments that are routinely used to determine the structure of macromolecules [41, 73]. On the other hand, in the solid phase, the direct spin-spin interaction (also known as dipolar coupling or through-space interaction) dominates the CT process between nuclei. Indeed, the heteronuclear dipolar coherence transfer is often employed in solid phase experiments to enhance the sensitivity of low  $\gamma$  nuclei and/or low natural abundance nuclei [74]. Generally, homonuclear dipolar-mediated coherence transfer (DCT) cannot be detected in isotropic solutions because random rotational motion of molecules averages out the dipolar couplings, even though incoherent magnetization transfer is still possible, resulting in efficient relaxation [73]. In most static solids, except uniaxially oriented solids, overlap of broad spectral lines complicates the study of DCT.

In magic-angle spinning experiments, selective recovery of the homonuclear spin-1/2 dipolar coupling and the measurement of coherent homonuclear DCT are possible using specific pulse sequences [36-38, 56-58, 75-101]. The strong distance dependence of DCT makes the quantification of this effect attractive for use as a distance measurement tool. An understanding of these exchange modes can aid in the design of multiple-pulse sequences to assure the greatest transfer of coherence from a specific spin at a certain experimental time. In fact, solid-state NMR techniques designed based on the

concept of DCT are routinely used to provide interatomic distance information in macromolecules (samples excepting isotropic liquids), such as crystalline polymers, liquid crystals, fibrous biopolymers, peptides or proteins in cell membranes, and other biological solids [24, 27, 69, 102-114] .

Further experimental design of pulse sequences requires a theoretical treatment of DCT in various systems, which must be laid as groundwork for more complex collection of spins. Because of the nature of the dipolar interaction between like spins, analytical solutions to homonuclear coherence transfer prove to be complex even for simple two spin systems. Previous publications have done much to clarify the strong and weak coupling effects on the spectral features of homonuclear spin  $\frac{1}{2}$  dipolar-coupled systems [91, 92]. In this paper, we will employ theoretical tools to explore the modes of homonuclear DCT in a uniaxially oriented or single crystal solid-state system, consisting of two-spin  $\frac{1}{2}$  homonuclei.

## Theory

Consider a two chemically inequivalent homonuclear spin  $\frac{1}{2}$  nuclei in a uniaxially oriented or a single crystal sample. We assume that the dipolar coupling as well as the scalar coupling between the two nuclei is nonzero. Further, relaxation effects are ignored in the present theoretical study. The total Hamiltonian for this system in the presence of a static external magnetic field consists of chemical shift, scalar coupling, and dipolar coupling terms:

$$H_T = H_D + H_{CS} + H_J \quad (3-1)$$

We assume that an experimental situation can be created to selectively suppress the chemical shift interaction with minimal or no effect on the coupling terms of the total Hamiltonian  $H_T$ . Then the total Hamiltonian in Eq. 3-1 becomes the sum of  $H_D$  and  $H_J$ .

Henceforth, we refer to this total Hamiltonian ( $H_T$ ) as the coupling Hamiltonian ( $H_{JD}$ );  $H_T = H_D + H_J = H_{JD}$ .

This Hamiltonian is equivalent to the creation of a zero-field or rotating-frame Hamiltonian in a solid-state NMR experiment. A simple spin echo sequence, in the form of a series of  $180^\circ$  pulses, can be used to refocus the chemical shifts and leave the scalar as well as the dipolar couplings unaltered. On the other hand, a multiple RF pulse sequence can be used to spin lock as well as scale the homonuclear dipolar coupling. For example, consider a multiple RF pulse sequence consisting of a spin echo sequence for one half of the cycle and magic echo sequence for the second half of the cycle. It can be shown using the average Hamiltonian theory that the effective Hamiltonian of this unified spin echo and magic echo (USEME) [58] pulse sequence is  $0.5H_D + H_J$ . The spin echo sequence, consisting of a series of  $\pi$ -pulses, suppresses the chemical shift interaction and leaves the dipolar and scalar couplings unaltered. On the other hand, the magic echo sequence suppresses the chemical shift interaction, scales the dipolar coupling interaction by a factor of 20.5, and leaves the scalar couplings unaltered. Thus, a complete cycle of USEME suppresses the chemical shift interaction, scales the dipolar coupling interaction by a factor of 10.5, and leaves the scalar couplings unaltered. Therefore, a solid-state NMR experiment can be designed to study the coherence transfer between two coupled (dipolar as well as scalar) spin 1/2 nuclei in a uniaxially oriented or a single crystal system. Such a study will be useful in measuring the orientation of the chemical bond or a peptide plane in order to determine the backbone conformation of polypeptides embedded in phospholipid bilayers. For example, the coupling  $^{13}\text{C}_\alpha-^{13}\text{C}_\text{O}$  parameter can be measured on uniaxially oriented biological solids.

In this paper, coherence transfer modes are analyzed under the total coupling Hamiltonian,  $H_{JD}$ . In static solids, usually the scalar coupling term,  $H_J$ , is smaller in magnitude than the dipolar coupling term and is often neglected. The scalar coupling becomes important in oriented solid-phase samples especially when the homonuclear

dipolar coupling is small. Therefore, the effect of the scalar coupling on CT via the dipolar coupling is included in our calculations. The dipolar coupling Hamiltonian can be expressed in the form of spherical tensors,

$$H_D = \sum_{q=-2}^{+2} (-1)^q D_{2q} T_{2-q} \quad (3-2)$$

where the second-rank tensors  $D_{2q}$  and  $T_{2-q}$  define the spatial and spin parts of the dipolar coupling Hamiltonian. The secular dipolar coupling Hamiltonian can be given as [60]

$$H_D = \frac{\hbar \gamma_I \gamma_S}{4 \pi r_{IS}^3} [1 - 3 \cos^2 \theta] (3I_z S_z - I \cdot S) \quad (3-3)$$

where  $\theta$  is the angle between the magnetic field and the vector connecting the two spins,  $r_{IS}$  is the distance between I and S nuclei, and  $\gamma_i$  is the gyromagnetic ratio of nucleus I [60]. Since the structure of the direct and indirect coupling Hamiltonians for a homonuclear spin system is similar, the total coupling Hamiltonian is given as

$$H_{JD} = (2D_{IS} + J)I_z S_z - (D_{IS} + J)\{I_x S_x + I_y S_y\} \quad (3-4)$$

where J is the scalar-coupling constant and  $D_{IS}$  is the dipolar coupling defined as

$$D_{IS} = \frac{\hbar \gamma_I \gamma_S}{4 \pi r_{IS}^3} [1 - 3 \cos^2 \theta] \quad (3-5)$$

In order to evaluate the coherence transfer modes due to the evolution under the coupling Hamiltonian, we assume a uniaxially oriented system with  $\theta = 0^\circ$ . Any change in the value of  $\theta$  will only change the magnitude of the  $D_{IS}$  parameter.

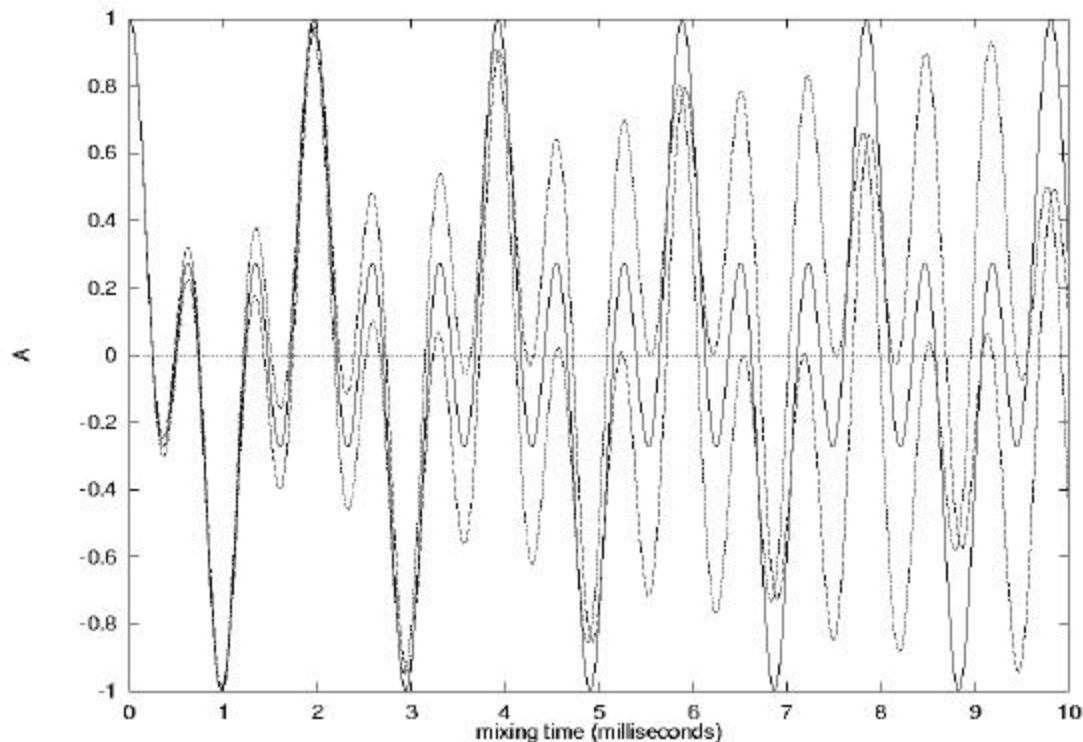


**Figure. 3-1** (a-g, this and subsequent pages): Expectation values of various spin operators under the dipolar coupling Hamiltonian,  $H_D$  (solid lines), and the total coupling Hamiltonian,  $H_{JD}$  (dotted and dashed lines). The coefficients of the spin operators given in Table 2-1 are plotted as a function of evolution time in an oriented or single crystal system containing two  $^{13}\text{C}$  nuclei separated by a distance of  $1.55 \text{ \AA}$ . The dotted lines are for  $J = -53 \text{ Hz}$  and the dashed lines are for  $J = 53 \text{ Hz}$ . For example, in (a), the magnitude of the term A is plotted as a function of the evolution time under the Hamiltonian  $H_{JD}$ . This can be used to evaluate the amount of magnetization which remains in the source or in I nuclei when x magnetization of the I nuclei is selected for the coherence transfer under the coupling Hamiltonian. Similarly, in (b), the magnitude of the term B is plotted as a function of the evolution time under the Hamiltonian  $H_{JD}$ . This can be used to evaluate the amount of magnetization transferred to the S nuclei when x magnetization of the I nuclei is selected for the coherence transfer under the coupling Hamiltonian.

Figure 3-1b

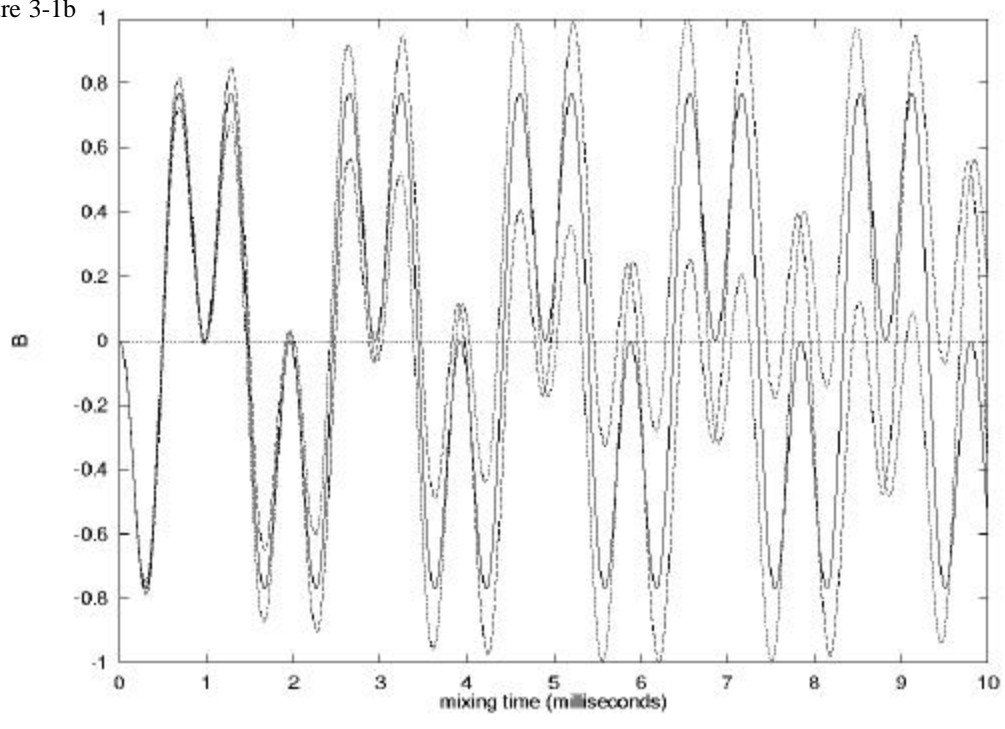


Figure 3-1c

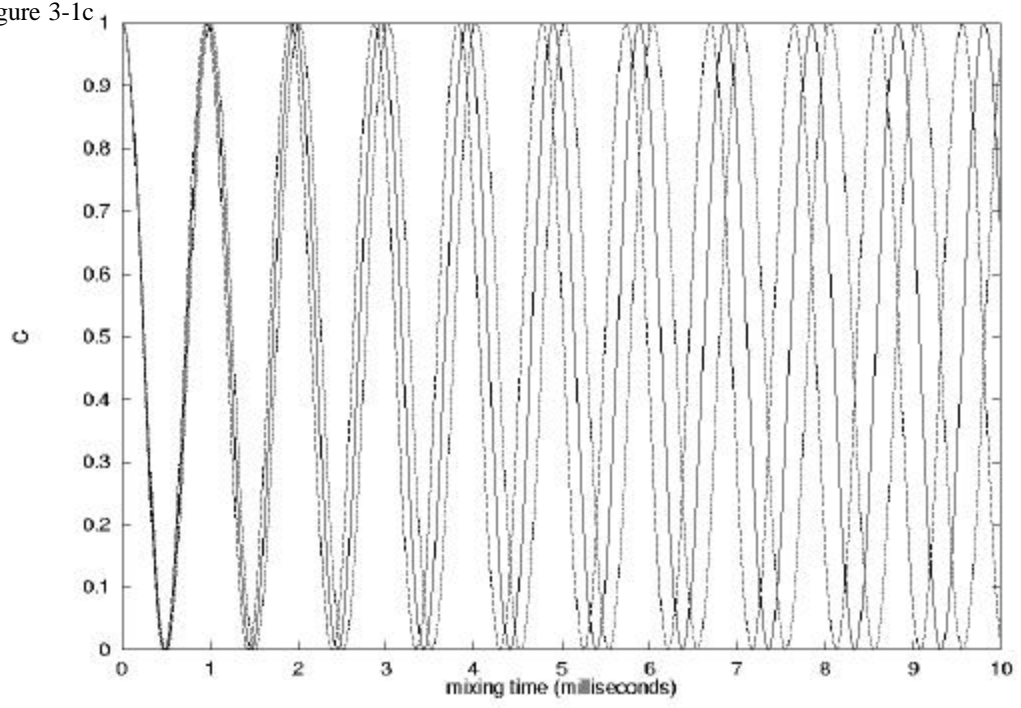


Figure 3-1d

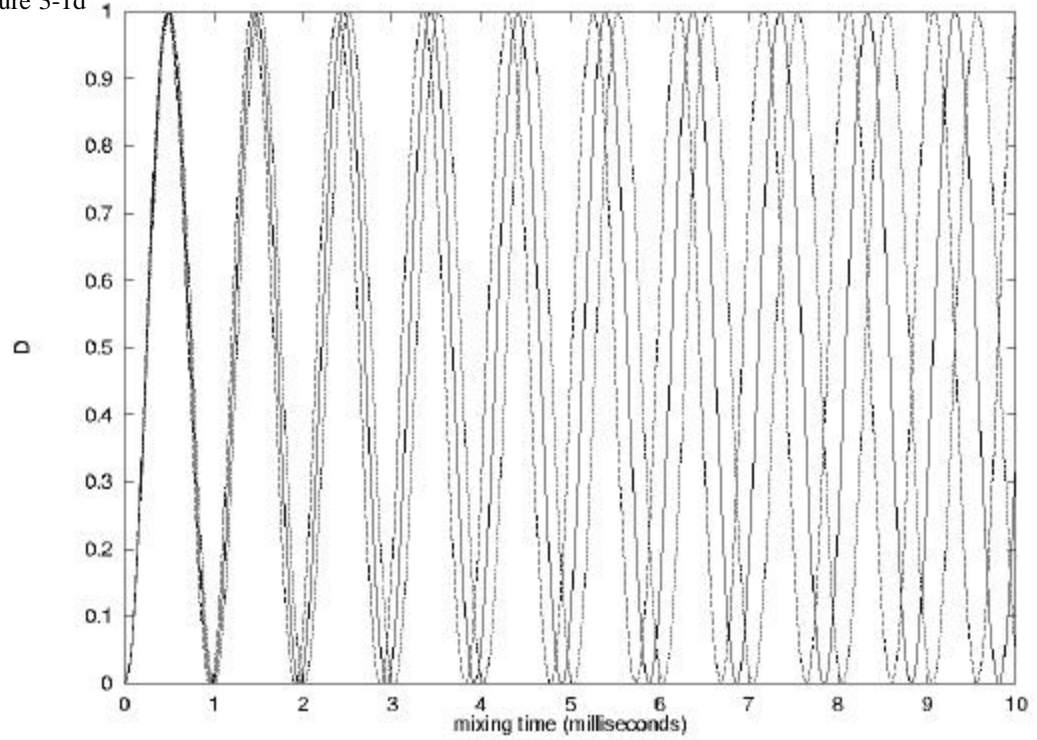


Figure 3-1e

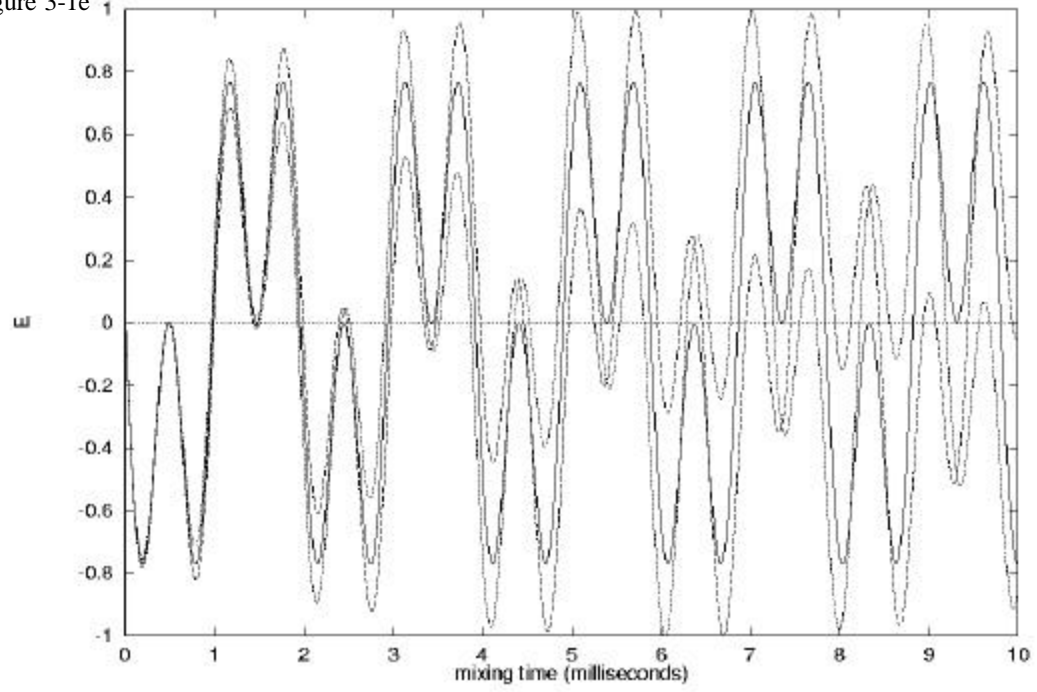




Figure 3-1f<sub>1</sub>

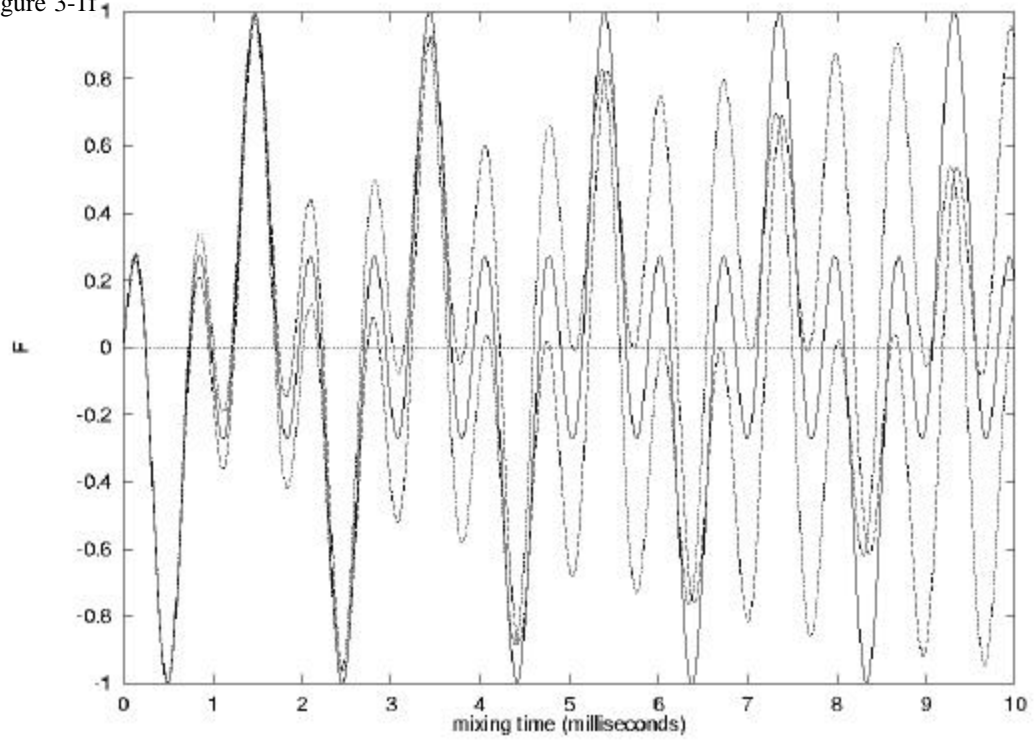
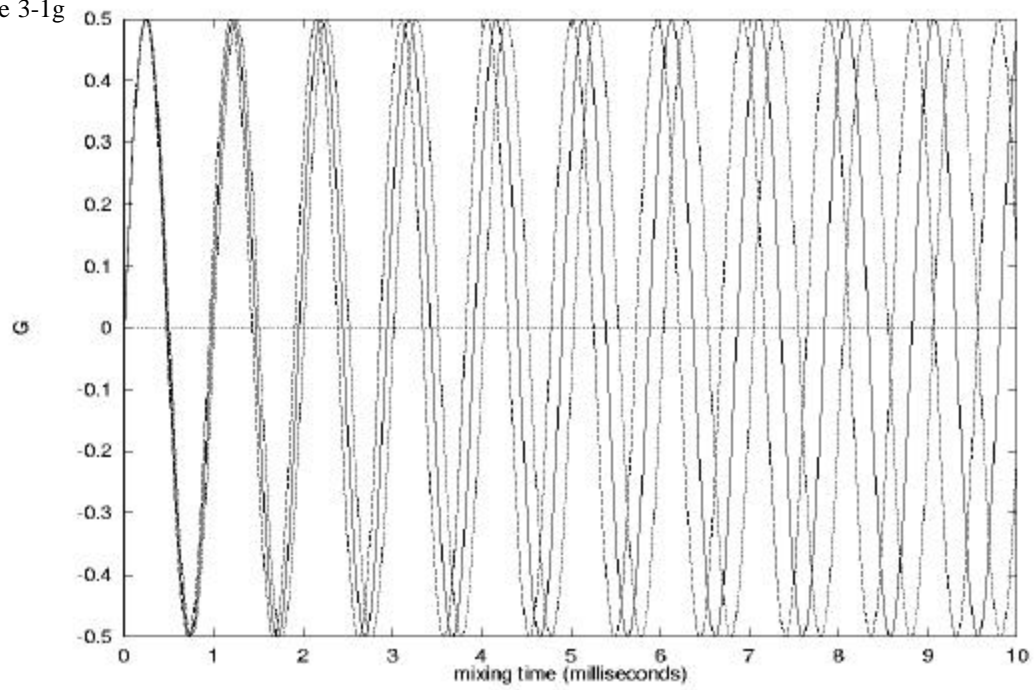


Figure 3-1g



## Results and Discussion

The evolution of all the spin operators that span the two-spin space under the coupling (both scalar and dipolar) Hamiltonian (see Eq. 3-4) is evaluated and the results are summarized in Tables 1 and 2. The spin part of the total coupling Hamiltonian,  $H_{JD}$ , is composed of a term  $IzSz$ , identical to the weak scalar coupling Hamiltonian, and a term  $\mathbf{I}\mathbf{S}$ , identical to the strong scalar coupling Hamiltonian. Since these two terms commute, the evolutions under both these terms were sequentially carried out in the calculations.

Further, the calculations are simplified because the product operators in  $\mathbf{I} \cdot \mathbf{S}$  commute with each other. Since the operators  $IzSz$ ,  $IySy$ , and  $IxSx$  commute with  $H_{JD}$ , they have a constant of motion under  $H_{JD}$ , and therefore they are not given in Table 3-1. In other words, the expectation values of the spin operators are summarized in Table 3-1 for an evolution of a two homonuclear spin-1/2 system under the coupling Hamiltonian  $H_{JD}$ .

An initial state of the spin system is specified in the first column of Table 3-1 and the coefficients of the product operators in the final density matrix are given in the subsequent columns of Table 3-1. For example, the evolution of the initial density matrix representing the x magnetization of the nuclei I, the  $I_x$  operator, under  $H_{JD}$  is given as

$$I_x \xrightarrow{H_{JD}} \frac{1}{2} \begin{pmatrix} I_x(\cos(\alpha pt) + \cos(\beta pt)) \\ -I_y S_z (\sin(\alpha pt) + \sin(\beta pt)) \\ + I_z S_y (\sin(\alpha pt) - \sin(\beta pt)) \\ + S_x \sin(\gamma pt) \end{pmatrix} \quad (3-6)$$

The angles  $\alpha$ ,  $\beta$ , and  $\gamma$  are defined in Table 3-2. This equation can be realized by reading across the row of Table 3-1. This corresponds to the selective preparation of the x magnetization of the I nuclear spins, then allowing an evolution under a specifically designed RF pulse sequence that leaves the coupling Hamiltonian unaltered in an experiment. It is clear from Eq. 3-6 that the evolution of the  $I_x$  operator under  $H_{JD}$  leads

to  $I_x$ ,  $S_x$ ,  $I_yS_z$ , and  $I_zS_y$  operators. In other words, the observable x magnetization of an I nuclear spin (as  $I_x$ ) is transferred as the observable x magnetization of S nuclear spin (as  $S_x$ ), as well as antiphase I (as  $I_yS_z$ ) and S (as  $I_zS_y$ ) magnetizations. The expectation values of  $I_x$ ,  $S_x$ ,  $I_yS_z$ , and  $I_zS_y$  operators for the evolution of the  $I_x$  operator under the Hamiltonian  $H_{ID}$  is given by the terms A, B, 2E, and F, respectively.

The coefficients of the product operators are plotted as a function of the evolution time in Fig. 3-1 for a  $^{13}\text{C}-^{13}\text{C}$  system with a dipolar coupling  $D_{CC} = 2203.8$  Hz corresponding to a distance  $r_{CC} = 1.55$  Å. These data represent the distance and the dipolar coupling between the directly bonded  $^{13}\text{C}\alpha$  and  $^{13}\text{C}_O$  nuclei in the backbone of a peptide. Analysis of the Fourier transform of these time domain functions yields spectra that consist of dipolar as well as scalar coupling information. In Fig. 3-1, the evolution of spin operators is represented in solid, dotted, and dashed lines for  $J = 0$ ,  $J = -53$ , and  $J = 53$  Hz, respectively. For example, in Fig. 3-1a, the magnitude of the term A is plotted as a function of the evolution time under the Hamiltonian  $H_{ID}$ . This function can be used to evaluate the amount of magnetization that remains in the source (or in the I nuclei) when the x magnetization of the I nuclei is selected for the coherence transfer under the coupling Hamiltonian  $H_{ID}$ . Similarly, in Fig. 3-1b, the magnitude of the term B is plotted as a function of the evolution time under the Hamiltonian  $H_{ID}$ . This function can be used to evaluate the amount of magnetization transferred to the S nuclei when x magnetization of the I nuclei is selected for the coherence transfer under the coupling Hamiltonian  $H_{ID}$ .

The evolution of spin operators under any one of the coupling Hamiltonians ( $H_D$  or  $H_J$ ) can easily be separated using the results from Tables 3-1 and 3-2. It can be seen from Eq. 3-6 that the dipolar coupling Hamiltonian leads to in-phase as well as antiphase transfer of magnetization like the scalar coupling Hamiltonian. The in-phase transfer of x magnetization can be understood from Figs. 3-1a and 3-1b. Even though the transfer of a transverse magnetization via  $H_D$  and  $H_J$  appears to be similar, the evolution

**Table 3-1:** Expectation values of operators evolving under the dipolar and scalar coupling Hamiltonians. The initial states are given in the leftmost column. The evolving states are to be read across the row. For instance,  $I_x$  evolves to  $A I_x + B S_x - E I_y S_z + F I_z S_y$ . The values of A-G are given in Table 2.

$s(t) \downarrow$	$I_x$	$S_x$	$I_y$	$S_y$	$I_z$	$S_z$	$2I_x S_y$	$2I_y S_x$	$2I_x S_z$	$2I_z S_x$	$2I_y S_z$	$2I_z S_y$
$I_x$	A	B									-E	F
$S_x$	B	A									F	-E
$I_y$			A	B					E	-F		
$S_y$			B	A					-F	E		
$I_z$					C	D	-G	G				
$S_z$					D	C	G	-G				
$2I_x S_y$					G	-G	C	D				
$2I_y S_x$					-G	G	D	C				
$2I_x S_z$			-E	F					A	B		
$2I_z S_x$			F	-E					B	A		
$2I_y S_z$	E	-F									A	B
$2I_z S_y$	-F	E									B	A

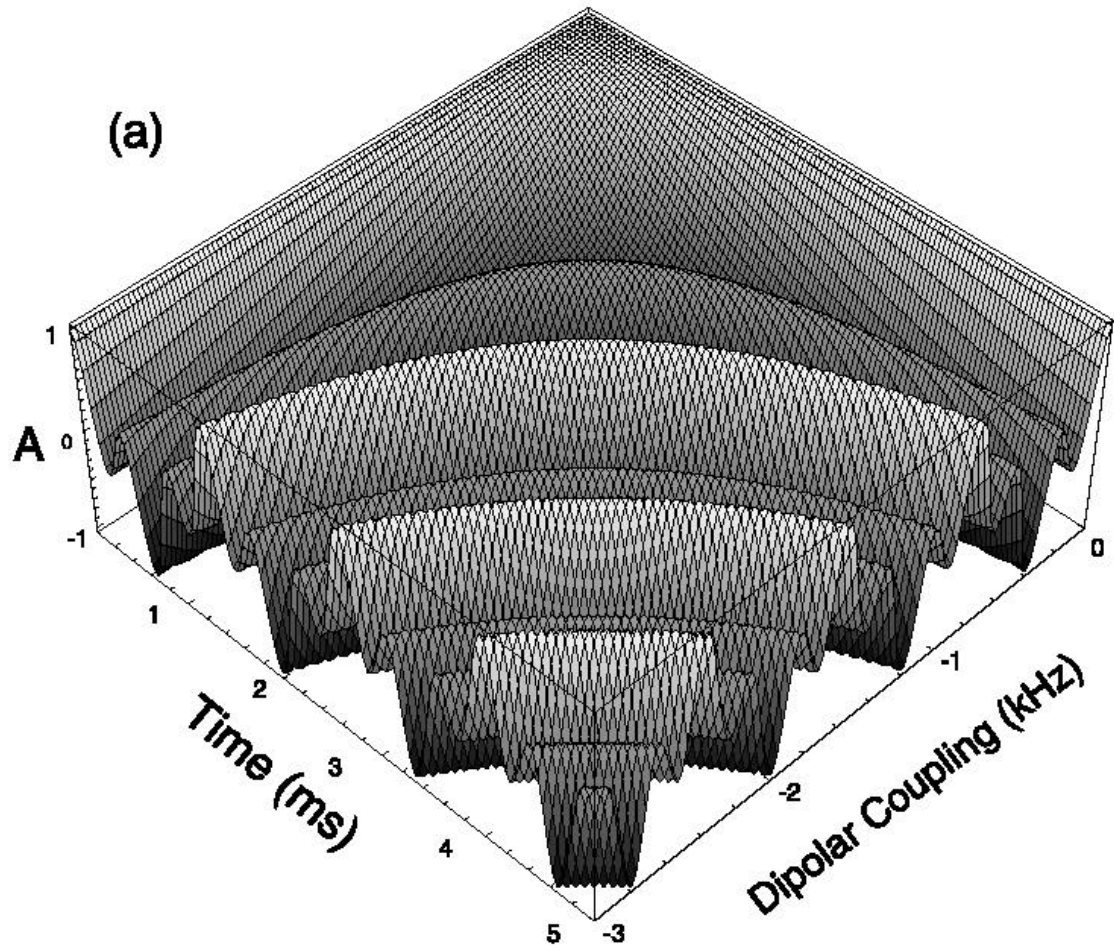
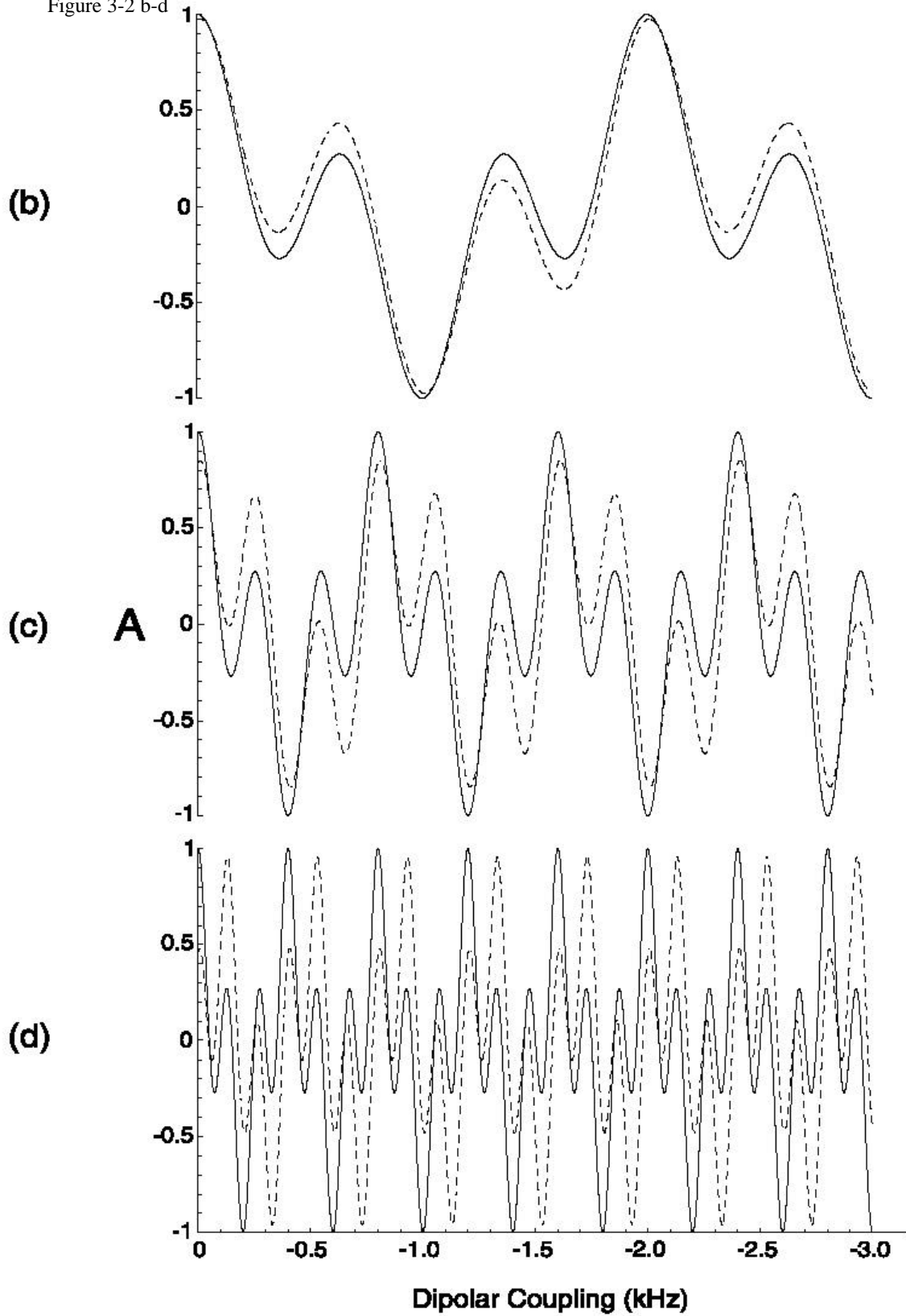


**Figure 3-2** (this and following page) (a) Three-dimensional plot showing the dependence of the expectation value of the  $I_x$  operator during the evolution of the  $I_x$  operator under the HD Hamiltonian (as given by the term A in Table 1) on the dipolar coupling and the evolution time. Two-dimensional slices (b), (c), and (d) taken from the three-dimensional plot in (a) for the evolution times 2, 5, and 10 ms, respectively, are shown for  $J = 0$  (solid lines) and for  $J = 53$  Hz (dashed lines).

of the spin operators are different for both cases. In the case of the  $H_J$  mixing Hamiltonian, the active frequencies in the evolution are the same, that is,  $J$ , for all spin operators. But in the case of the  $H_D$  mixing Hamiltonian, the evolution frequencies are a combination of two different frequency terms,  $0.5 \pi D_{IS}$  and  $1.5 \pi D_{IS}$ , for all spin operators as seen from the expressions for A, B, E, and F in Table 2. It may be noted that the evolutions of x and y magnetizations under the total coupling Hamiltonian  $H_{JD}$  or under the individual coupling Hamiltonians ( $H_D$  or  $H_J$ ) are similar as seen from Tables 3-1 and 3-2 and Fig. 3-1.

Figure 3-2 b-d



As shown in Table 2-1 and Fig. 1, the evolution of antiphase product operators,  $I_p S_q$  and  $I_q S_p$  ( $p = x$  or  $y$ ;  $q = z$ ), is similar to that of  $I_p$  ( $p = x$  or  $y$ ) operators. They lead to in-phase  $x$  or  $y$  magnetization in addition to antiphase product operators. This suggests that the antiphase multiplet signal can be refocused into an in-phase multiplet for detection just like RINEPT experiments [41, 115] for a weakly scalar coupled spin system in isotropic solutions. This strategy will be highly valuable as the broad lines of

Table 3-2  
Coefficients of the Spin Operators Generated Due to the Evolution under  $H_{JD}$  and Their First-Maxima and First-Zero

Coefficients of spin operators	Figure	First-maxima	First-zero
$A = 0.5(\cos \alpha \pi t + \cos \beta \pi t)$	1a	$-4/D_{IS}$	$-1/(2D_{IS})$
$B = 0.5(-\cos \alpha \pi t + \cos \beta \pi t)$	1b	*	$-1/D_{IS}$
$C = 0.5(1 + \cos \gamma \pi t)$	1c	$-2/D_{IS}$	$-1/D_{IS}$
$D = 0.5(1 - \cos \gamma \pi t)$	1d	$-1/D_{IS}$	$-2/D_{IS}$
$E = 0.5(\sin \alpha \pi t + \sin \beta \pi t)$	1e	*	$-1/D_{IS}$
$F = 0.5(\sin \alpha \pi t - \sin \beta \pi t)$	1f	$-3/D_{IS}$	$-1/(2D_{IS})$
$G = 0.5(\sin \gamma \pi t)$	1g	$-1/(2D_{IS})$	$-1/D_{IS}$

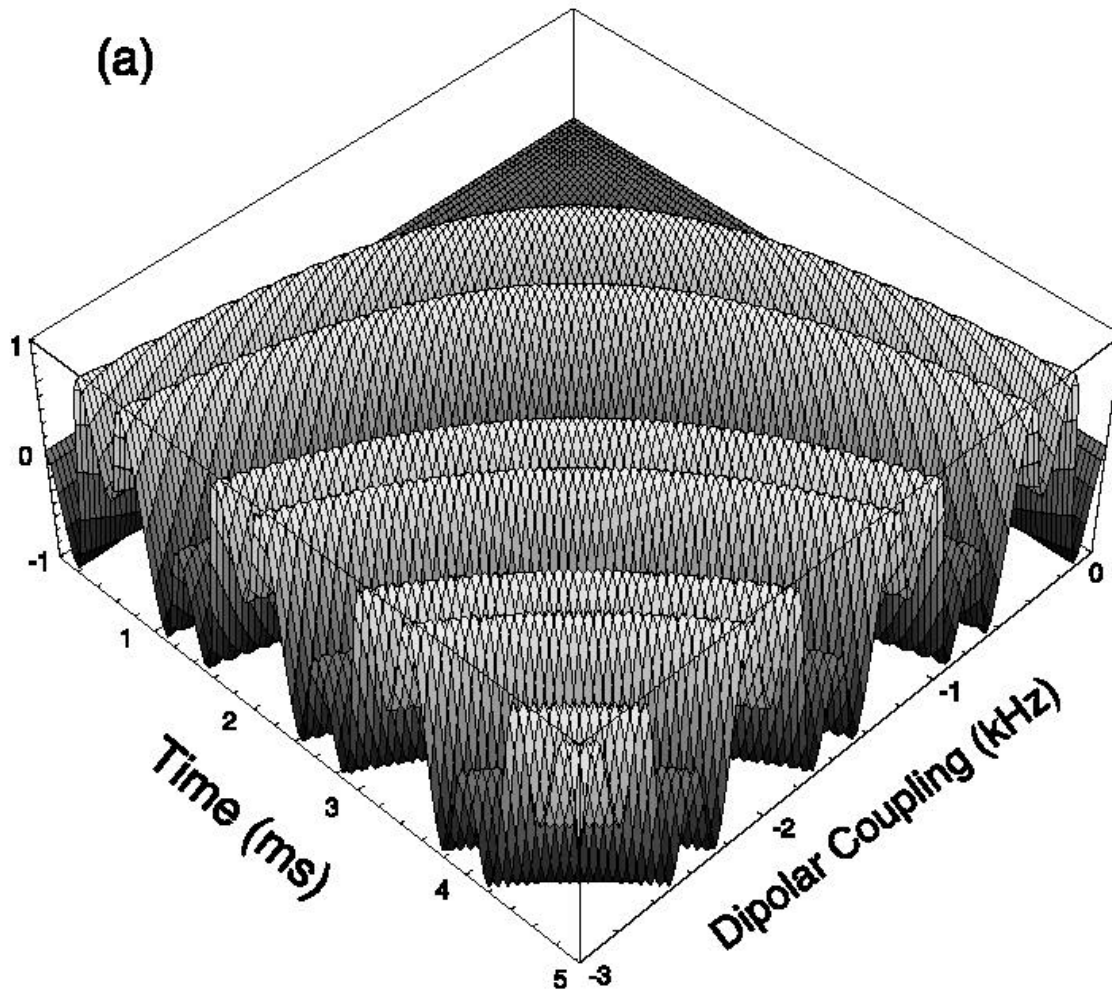
Note. \* No analytical solution was found.  $\alpha = (D_{IS}/2 + J)$ ;  $\beta = (3D_{IS}/2)$ ;  $\gamma = (J - D_{IS})$ ;  $D_{IS} = -\hbar \gamma_I \gamma_S / 2 \pi r_{IS}^3$ .

the antiphase doublet in solids will be difficult to observe, especially when the dipolar coupling is small. The evolution times under the coupling Hamiltonian for the maximum conversion of  $I_x$  into  $I_z S_y$ ,  $S_x$  into  $I_y S_z$ ,  $I_y$  into  $-I_z S_x$ ,  $S_y$  into  $-I_x S_z$ ,  $I_z S_y$  into  $-I_x$ ,  $I_y S_z$  into  $-S_y$ ,  $I_z S_x$  into  $I_y$ , and  $I_x S_z$  into  $S_y$  are the same as given by the term F in Fig. 1f. The evolution of the  $I_z$  (or  $S_z$ ) operator under  $H_D$  is significantly different from that of the transverse components,  $I_x$  (or  $S_x$ ) and  $I_y$  (or  $S_y$ ), unlike the case of  $H_J$  as can be seen from Tables 3-1, 3-2 and Fig. 3-1. This is mainly because the spin part of the dipolar coupling Hamiltonian that is operative on these angular momentum operators is different. They are  $3I_z S_z - I_y S_y$  for  $I_x$  (or  $S_x$ ),  $3I_z S_z - I_x S_x$  for  $I_y$  (or  $S_y$ ), and  $-I_x S_x - I_y S_y$  for  $I_z$  (or  $S_z$ ) since  $[I_i, I_i S_i] = 0$  and  $[S_i, I_i S_i] = 0$ . For the evolution of the  $I_z$  (or  $S_z$ ) operator under  $H_{JD}$ , the frequency of evolution of the spin operators in the final density matrix is  $\pi(J - D)$ . In fact, the transfer of  $z$  magnetization via  $H_D$ ,  $H_J$ , and  $H_{JD}$  is similar. They all yield an observable in-phase coherence transfer as well as an unobservable zero-quantum coherence (ZQC),  $I_x S_y - I_y S_x$ . The only difference is the rate of coherence

transfer. It is also to be noted that the evolution of the ZQC under the coupling Hamiltonians  $H_D$ ,  $H_J$ , and  $H_{JD}$  is similar. They all yield an observable z magnetization (see Table 3-1) but the only difference is the rate of coherence transfer. Therefore, any solution NMR methods that employ mixing of z magnetization or ZQC via the isotropic scalar coupling can either be adapted or suitably modified, depending on the strength of the homonuclear dipolar coupling, for solid-state NMR studies on uniaxially oriented systems. [9, 116, 117]

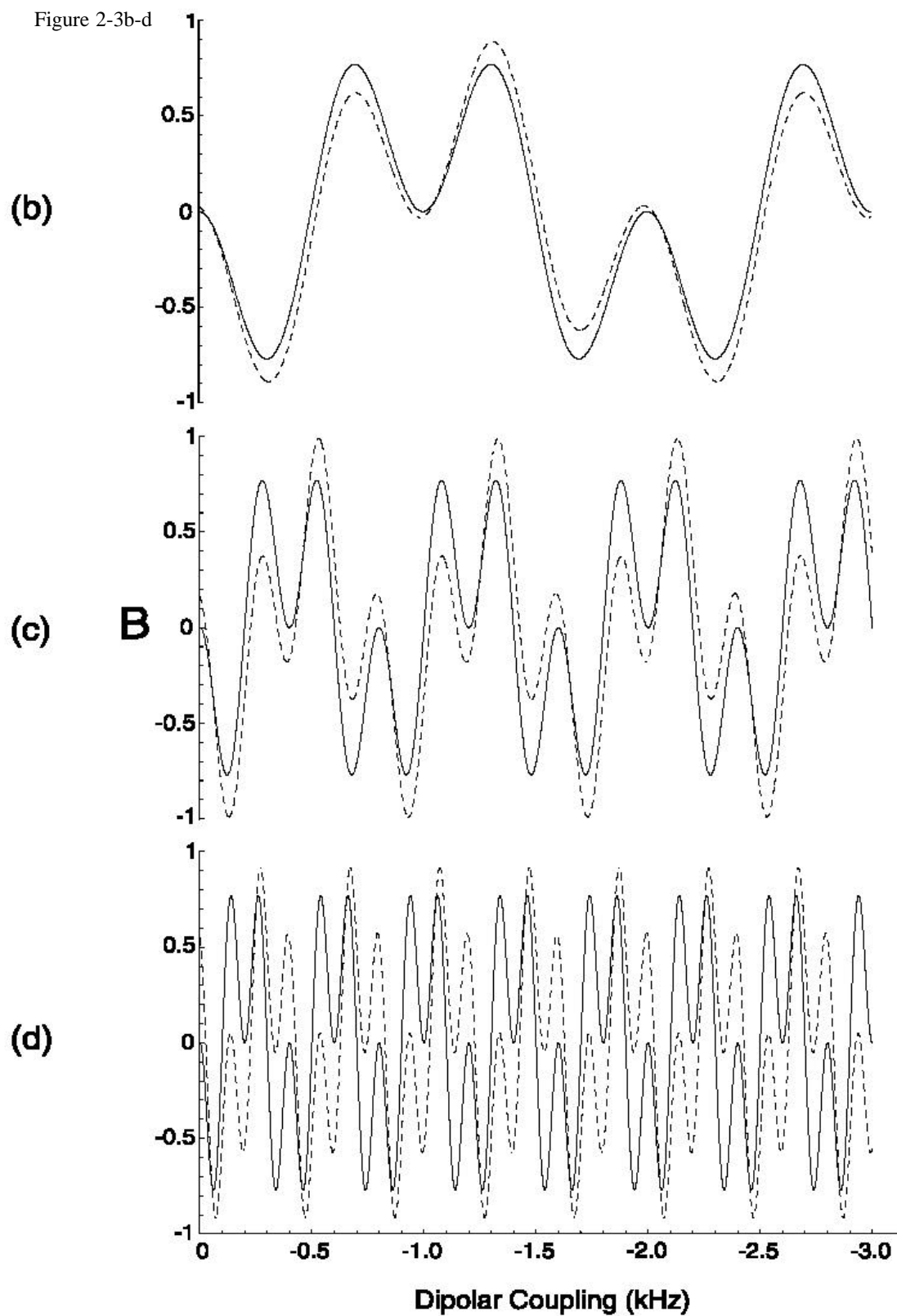
Although the structures of  $H_J$  and  $H_D$  Hamiltonians are similar, there is a significant difference between the coherence transfer via the scalar and the dipolar couplings. This is because the contribution to the CT process from the z component is different from that of the x and y components of the dipolar coupling Hamiltonian  $H_D$  unlike the case of the strong scalar coupling Hamiltonian  $H_J$ . In other words, evolution of the spin angular momentum operators under the strong scalar coupling Hamiltonian  $H_J$  leads to isotropic mixing, that is, all three components of the Hamiltonian  $H_J$  are equally operative, while evolution under the dipolar coupling Hamiltonian  $H_D$  leads to cylindrical mixing, that is, only two of the three components of the Hamiltonian  $H_D$  are equally operative. Therefore, the homonuclear dipolar coupling Hamiltonian  $H_D$  may be termed a cylindrical mixing Hamiltonian in analogy to the name isotropic mixing Hamiltonian for the strong scalar coupling Hamiltonian  $H_J$ . It should also be noted that the term  $I_i + S_i$  ( $i = x, y, z$ ) has a constant of motion under  $H_J$  while only the term  $I_z + S_z$  has a constant of motion under  $H_D$ . This suggests that a nonselectively prepared transverse magnetization in an experiment evolves under the influence of the dipolar coupling but not under the scalar coupling. It is interesting to note that a pair of chemically equivalent nuclei also evolves under the dipolar coupling during a spin-locking RF field as the  $I_z S_z$  term of  $H_D$  does not commute with the RF Hamiltonian, unlike in the case of scalar coupling.

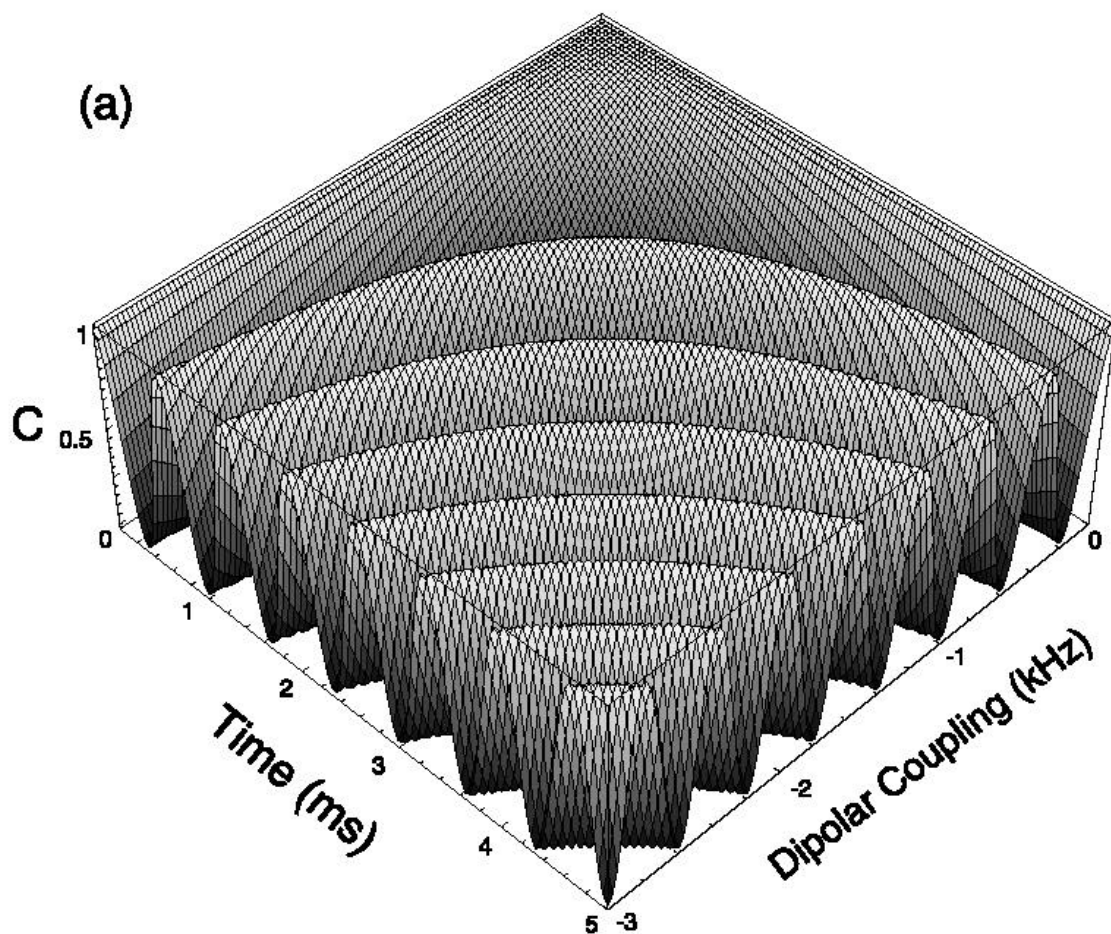




**Figure 3-3** (this and following page). (a) Three-dimensional plot showing the dependence of the expectation value of the  $S_x$  operator during the evolution of the  $I_x$  operator under the  $H_D$  Hamiltonian (as given by the term B in Table 1) on the dipolar coupling and the evolution time. Two-dimensional slices (b), (c), and (d) taken from the three-dimensional plot in (a) for the evolution times 2, 5, and 10 ms, respectively, are shown for  $J = 0$  (solid lines) and for  $J = 53$  Hz (dashed lines).system under the  $H_{JD}$  Hamiltonian. Two-dimensional slices in Figs. 3-2b to 3-2d are taken from the three-dimensional plot in Fig. 3-2a for various evolution times, while varying the dipolar coupling from 0 to 23 kHz. The dependence of the terms B, C, and D on the dipolar coupling and the evolution time are presented in Figs. 3-3, 3-4, and 3-5, respectively.

Figure 2-3b-d

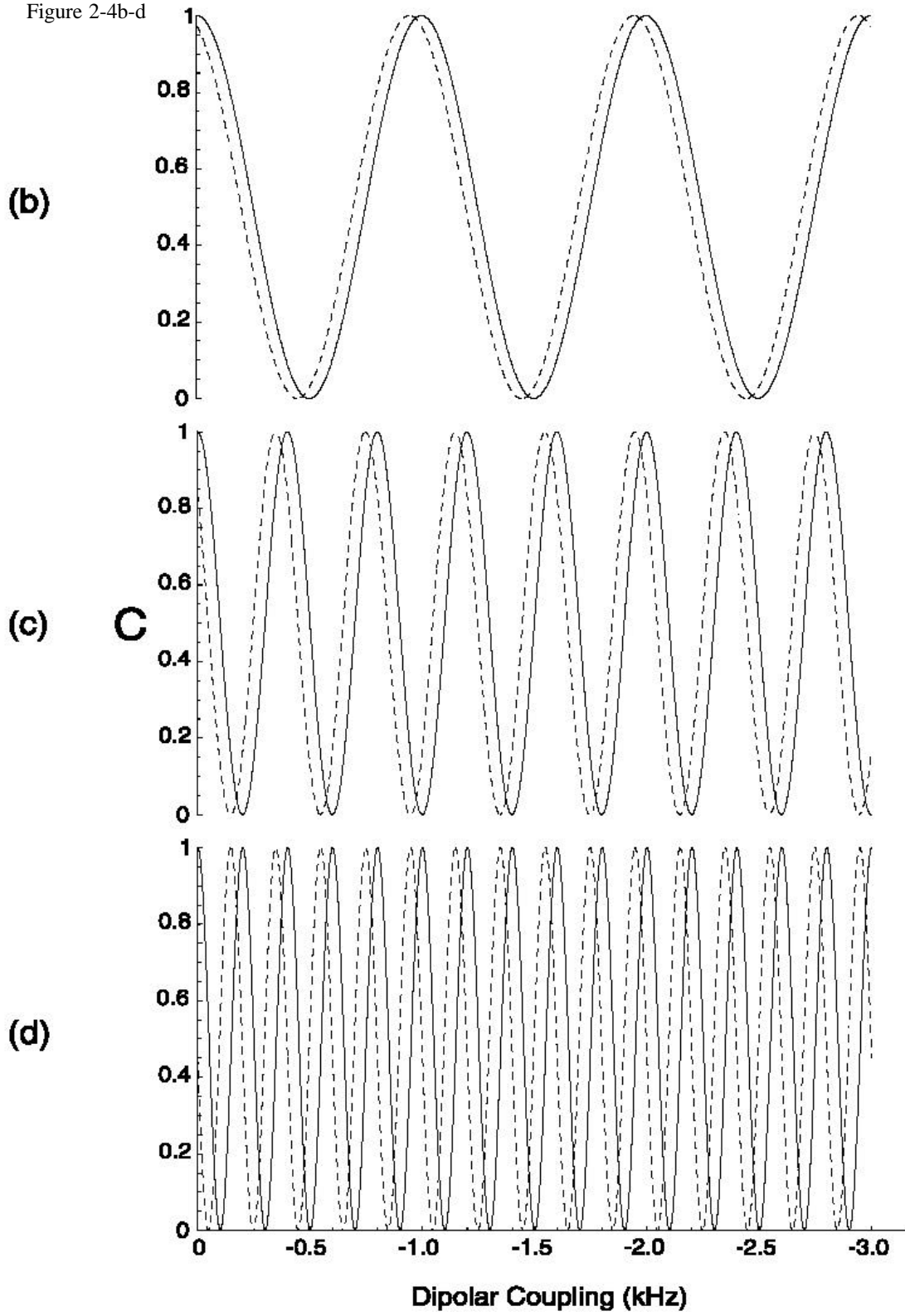


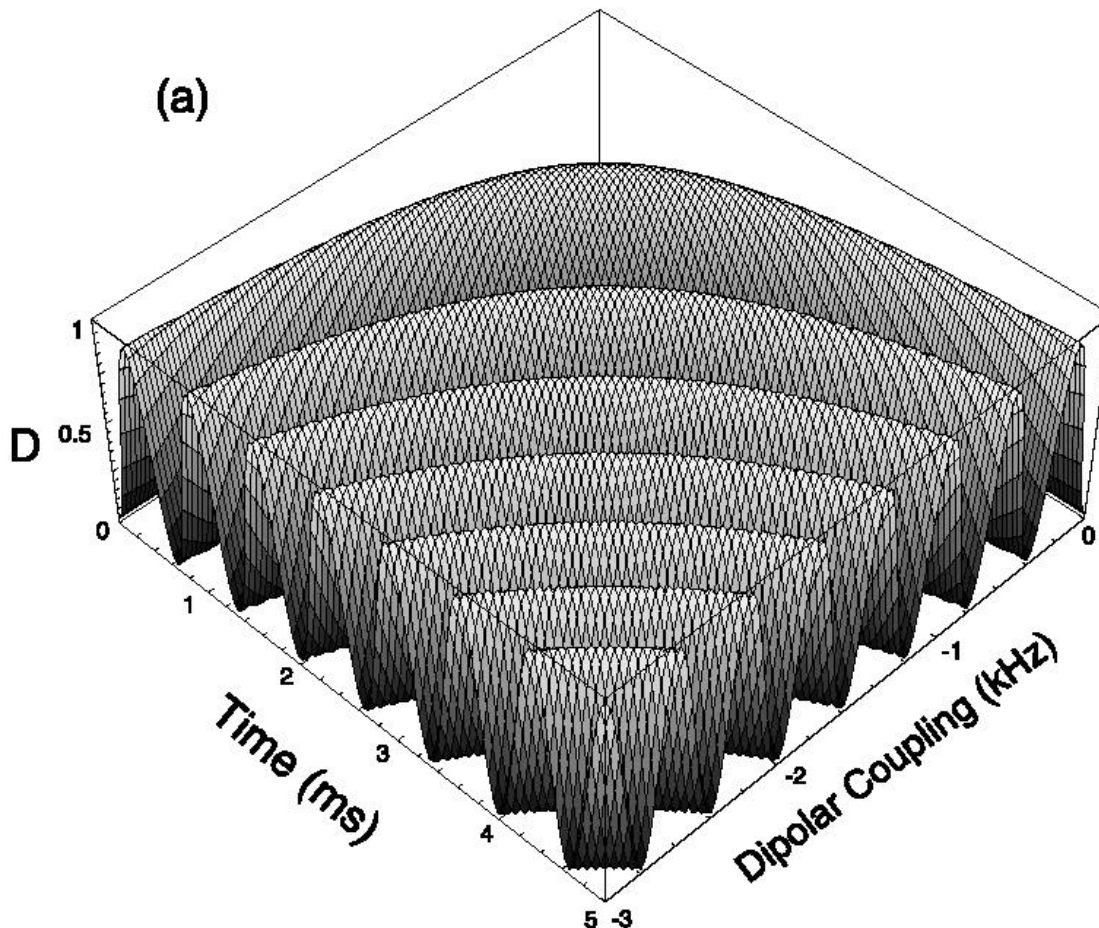


**Figure 3-4** (this and following page) (a) Three-dimensional plot showing the dependence of the expectation value of the  $I_z$  operator during the evolution of the  $I_z$  operator under the  $H_{JD}$  Hamiltonian (as given by the term C in Table 1) on the dipolar coupling and the evolution time. Two-dimensional slices (b), (c), and (d) taken from the three-dimensional plot in (a) for the evolution times 2, 5, and 10 ms, respectively, are shown for  $J = 0$  (solid lines) and for  $J = 53$  Hz (dashed lines).

It is evident from the two-dimensional plots (see Figures. 3-3 to 3-5) that the number of maxima of the terms A, B, C, and D against the dipolar coupling increases as a function of the evolution time. For example, in Fig. 3-2a, for an evolution time of 2 ms under a dipolar coupling of about 2.2 kHz, the transfer of x magnetization of the I nuclei to its dipolar-coupled partner is zero as can be seen from Figs. 3-2b and 3-3b. On the other

Figure 2-4b-d

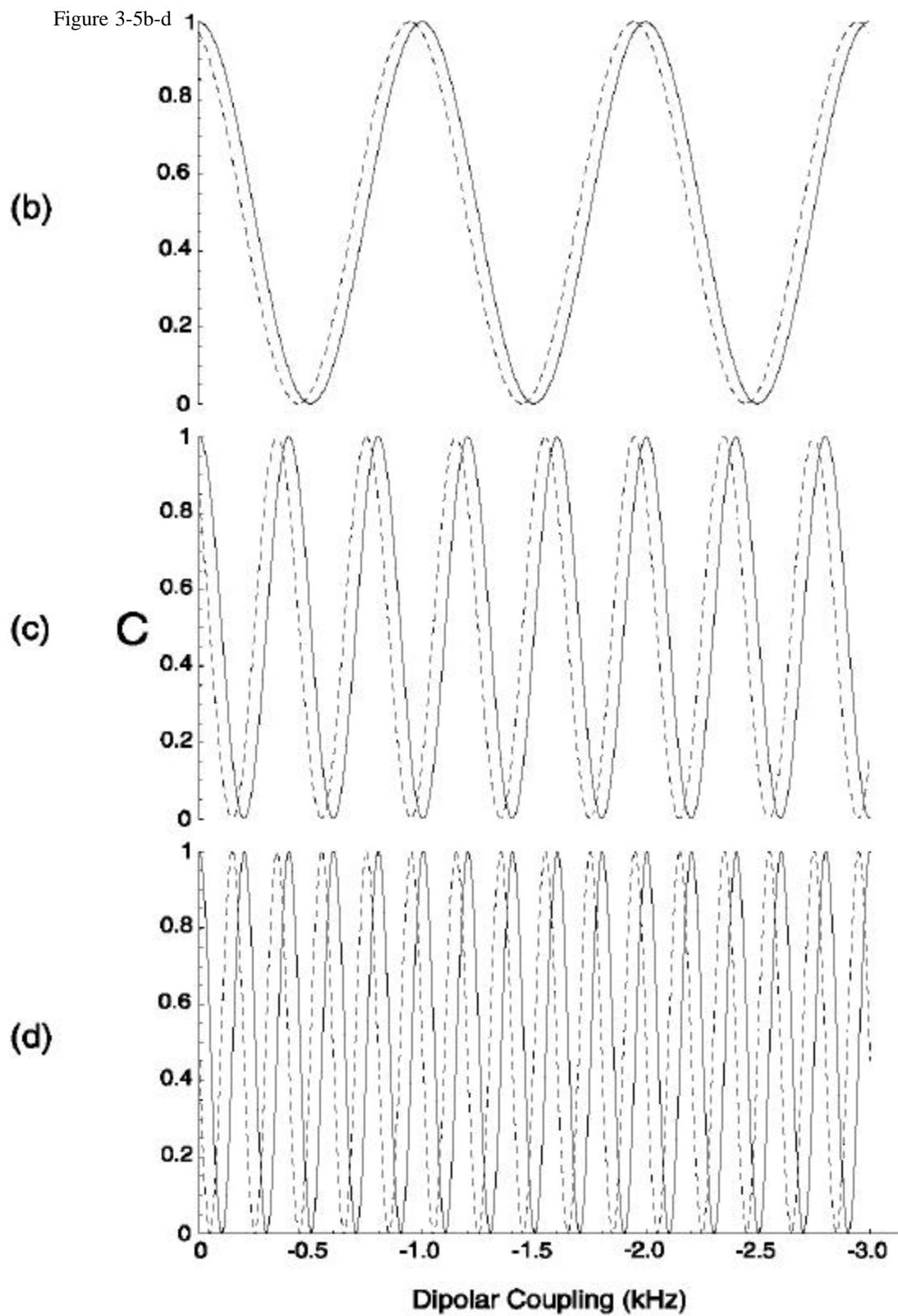




**Figure 3-5** (this and following page) (a) Three-dimensional plot showing the dependence of the expectation value of the  $S_z$  operator during the evolution of the  $I_z$  operator under the  $H_{JD}$  Hamiltonian (as given by the term  $D$  in Table 1) on the dipolar coupling and the evolution time. Two-dimensional slices (b), (c), and (d) taken from the three-dimensional plot in (a) for the evolution times 2, 5, and 10 ms, respectively, are shown for  $J = 0$  (solid lines) and for  $J = 53$  Hz (dashed lines).

hand, the maximum transfer occurs at a dipolar coupling of about 20.65 kHz (see Fig. 3-3b). It is interesting that  $I_x$  is transferred as  $\pm S_x$  depending on the magnitude of dipolar coupling and the evolution time. Therefore, care must be taken in quantifying the degree of DCT. The effect of the scalar coupling,  $J = 53$  Hz, is shown in dashed lines in Figs. (3-2) to (3-5). As the mixing time increases, the CT process is significantly dependent on the  $J$

Figure 3-5b-d



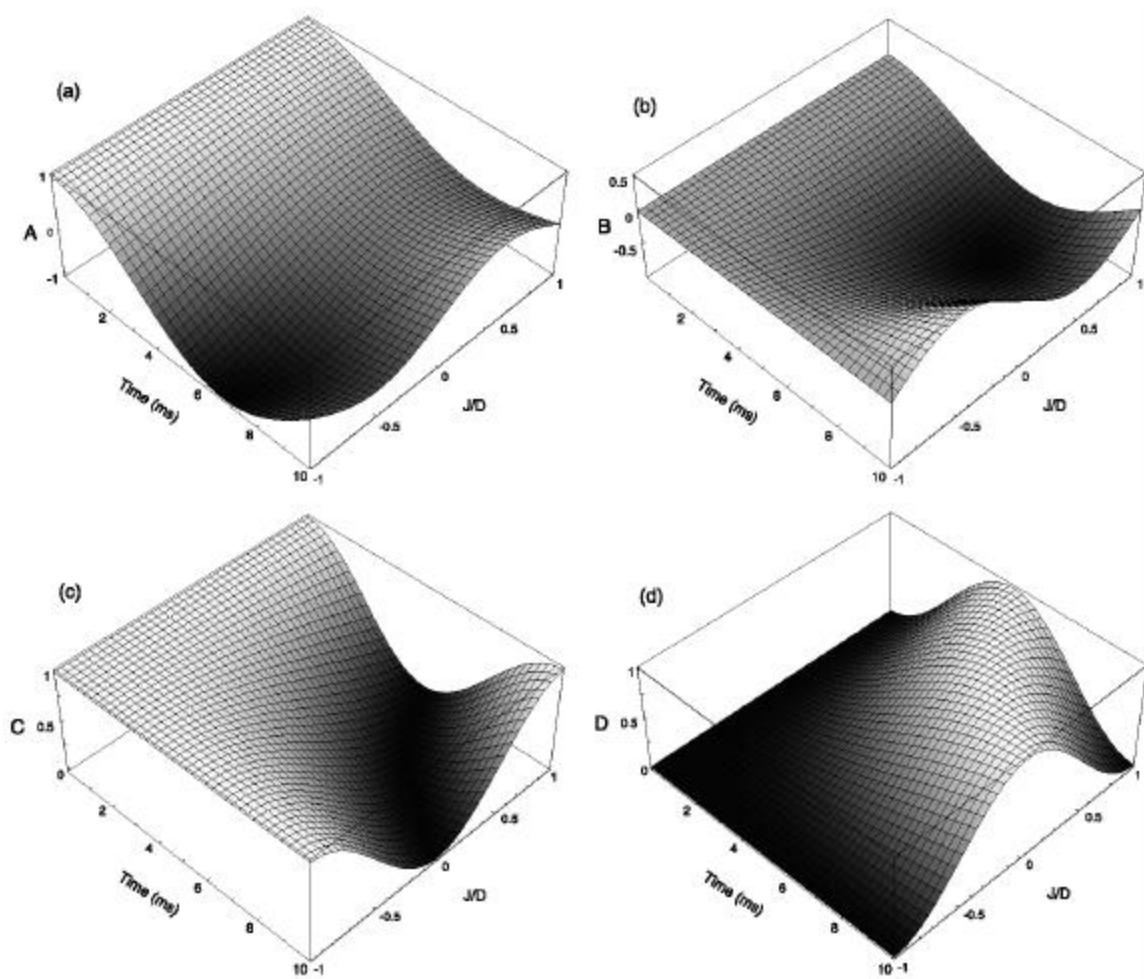


**Figure 3-6** Three-dimensional plots showing the dependence of the terms A, B, C, and D on the ratio of the scalar and dipolar couplings are shown in (a), (b), (c), and (d), respectively. The dipolar coupling was assumed to be 100 Hz.

parameter as evident from Figs. 3-2d, 3-3d, 3-4d, and 3-5d. First-maxima and first-zero of the coefficients of the spin operators are given in Table 3-2. The functions with no simple analytical solution for maxima are noted in the table. A nonzero scalar coupling not only changes the coherence transfer efficacy as indicated in Fig. 3-1 but also shifts the first-maxima and first-zero of the functions in Table 3-2. The presence of J makes it difficult to obtain an analytical solution for the first-maxima and first-zero for the CT process. Further, it is important to note that the absolute sign of J coupling changes the CT process as shown in Fig.3-1. These effects become significant if the dipolar coupling becomes smaller due to either the partial averaging of the dipolar coupling or the orientation of the dipole-dipole vector near the magic angle. Therefore care must be

taken in the experimental measurement of small dipolar couplings in order to obtain accurate interatomic distances. The dependence of the terms A, B, C, and D on the ratio of the scalar and dipolar couplings and on the evolution time is presented in Fig. 3-6. The results suggest that even small differences in the ratio of the couplings can make a significant difference in the CT efficacy.

## **Conclusions**

Coherence transfer under the dipolar coupling between a homonuclear spin-1/2 pair and the effects of the scalar coupling on DCT are analyzed in detail. The results suggest that DCT is a cylindrical mixing process unlike the isotropic mixing process under the strong scalar coupling Hamiltonian. The simple forms of the analytical equations that describe the coherence transfer under the dipolar coupling avail themselves to quick numerical simulations for experiments on oriented solid-state systems. It is clear that even small values of  $J$  compared to the dipolar coupling can make significant changes in the coherence transfer efficacy, and therefore the effect of  $J$  must be considered for the design of pulse sequences for the interatomic distance measurements and also to interpret the data from an oriented system, especially when the dipolar coupling is small. This may be significant in the study of partially oriented bicelles that are currently used to obtain large interatomic distance constraints for the structure determination of globular proteins using solution NMR methods. [8, 118, 119] Furthermore, the results from this work will be useful for designing experiments based on DCT, especially for the structural studies of uniaxially oriented biological solids [9, 116, 117] in solid-state NMR spectroscopy.



## **Acknowledgements**

Acknowledgment is made to the donors of the Petroleum Research Fund, administered by the American Chemical Society, for partial support of this research. D. M. Taylor acknowledges the Center for the Education of Women at the University of Michigan for the Margaret Dow Towsley Scholarship and for the Sloan Summer Fellowship.

**CHAPTER 4**  
**DIPOLAR-COUPPLING-MEDIATED COHERENCE TRANSFER IN AN**  
**UNORIENTED HOMONUCLEAR TWO SPIN- $\frac{1}{2}$  SOLID STATE SYSTEM**

**Abstract**

Homonuclear dipolar-coupling mediated coherence transfer (DCT), a through-space transfer of magnetization (or polarization or coherence) between like spins, can yield otherwise difficult-to-obtain structural information by measuring the internuclear distances between two specific sites of interest in a biological solid. Several RF pulse sequences under MAS are routinely used to measure the interatomic distances based on the recovered homonuclear dipole-dipole interaction. In this Chapter, DCT for a pair of dipolar coupled spin- $\frac{1}{2}$  nuclei in a powder sample is analyzed in detail, under static and MAS experimental conditions, by the numerical calculation of the analytical solutions for the time development of the density matrix. The density matrix evolution under the effect of the homonuclear dipolar interaction is evaluated using the product operator formalism. The effect of scalar coupling on DCT is also discussed in this Chapter. DCT in several dipolar-recoupling MAS experiments such as USEME, DRAWS, DRAMA, and RFDR are also analyzed. The behavior of DCT over a range of distances relevant to  $^{13}\text{C}$ -labeled peptides or proteins is presented, as well as an examination of the distance dependence of the maximum DCT over a range of mixing times for each of the experiments is presented.

## Introduction

Coherence transfer via the scalar coupling (through-bond or  $J$  coupling) is a basic concept successfully used in solution NMR experiments to determine the structure of macromolecules [41, 73]. In the solid phase, however, it is the dipolar coherence transfer (DCT), which modulates the majority of the coherence transfer between nuclei.

Heteronuclear DCT is often employed in solid-phase experiments such as the traditional cross-polarization (CP) method to enhance the sensitivity of low- $\gamma$  nuclei and/or low natural abundance nuclei [74].

In most static powder (or unoriented) samples, overlap of broad spectral lines due to anisotropic interactions complicates the study of DCT. The  $r^{-3}$  distance dependence of the dipolar interaction, even in unoriented samples, makes the quantification of this effect attractive for use as a distance measurement tool. Previous publications have done much to clarify the strong and weak coupling effects on the spectral features of homonuclear spin-1/2 dipolar-coupled systems [91, 92]. Magic-angle-spinning (MAS) experiments [73, 74] solve the problem of poor resolution caused by sample anisotropies. However, in doing so, the dipolar interaction among the low- $\gamma$  nuclei is also averaged to zero, so the distance information is lost in exchange for “solution-like” spectra.

Several recoupling pulse sequences have been developed to selectively recover the homonuclear spin-1/2 dipolar coupling (for example  $^{13}\text{C}$ - $^{13}\text{C}$  dipolar coupling) and are routinely used for the measurement of interatomic distances in proteins based on the homonuclear DCT process under MAS [36-38, 56-58, 76-103]. Therefore, a thorough analysis of DCT can aid in providing structural information for macromolecules (samples excepting isotropic liquids) such as unoriented samples of polymers, liquid crystals, peptides or proteins embedded in the cell membrane, fibrous proteins, and other unoriented or partially oriented biological [24, 27, 69, 103-114, 120]. In addition, such a

study is also important for the design of better dipolar recovery pulse sequences as well to refine, or to explore the limitations of, existing sequences.

Because of the nature of the dipolar interaction between like spins, analytical solutions to homonuclear DCT prove to be complex even for two-spin systems. Further understanding of DCT requires a theoretical investigation of simple two-spin systems in various experiments, which must be laid as groundwork for more complex collections of spins. In this paper, we will employ theoretical tools to explore various modes of homonuclear DCT in an unoriented solid-state system, consisting of two spin-1/2 homonuclei, both in a static powder and in the magic angle sample spinning dipolar recoupling (MASDR) experiments of USEME [58], RFDR [59], DRAMA[58] and DRAWS [57].

The main focus will be on various modes of coherence transfer as well as on the rate of coherence transfer via through space interaction, such as between directly bonded ( $H_{ID}$ , which includes both through bond and through space interactions) and approximately adjacent ( $H_D$ )  $^{13}C$  atoms in peptides.

In MASDR experiments, chemical shift (both isotropic as well as the anisotropic) interaction can contribute to the dephasing of a coherent signal. Experimental methods for reducing the contributions of the chemical shift in MASDR have been published by the original authors in many cases, and considerations and exceptions will be discussed in the text below. In this work, we consider DCT without explicit effects from a separate chemical shift term. In Chapter 5, we will include analysis of the effects of the chemical shift to the coherence transfer process.

### **Theory of the Static Dipolar Hamiltonian**

Consider two chemically inequivalent spin-1/2 nuclei in a sample consisting of randomly oriented polycrystallites. We assume that the dipolar coupling between the two